

Structural and kinetic effects of mobile phone microwaves on acetylcholinesterase activity

Mario Barteri^{a,*}, Alessandro Pala^b, Simona Rotella^a

^aDipartimento di Chimica- Università degli Studi di Roma “La Sapienza” Piazzale Aldo Moro 5 - 00185 Roma, Italy

^bLaboratorio di Biochimica degli Ormoni Sessuali,

Clinica Ostetrica e Ginecologica Università degli Studi di Roma “La Sapienza” Piazzale Aldo Moro 5 - 00185 Roma, Italy

Received 31 July 2004; received in revised form 21 September 2004; accepted 21 September 2004

Available online 18 October 2004

Abstract

The present study provides evidence that “in vitro” simple exposure of an aqueous solution of electric eel acetylcholinesterase (EeAChE; EC 3.1.1.7.) to cellular phone emission alters its enzymatic activity. This paper demonstrates, by combining different experimental techniques, that radio frequency (RF) radiations irreversibly affect the structural and biochemical characteristics of an important CNS enzyme. These results were obtained by using a commercial cellular phone to reproduce the reality of the human exposition. This experimental procedure provided surprising effects collected practically without experimental errors because they were obtained comparing native and irradiated sample of the same enzyme solution. Although these results cannot be used to conclude whether exposure to RF during the use of cellular phone can lead to any hazardous health effect, they may be a significant first step towards further verification of these effects on other “ex vivo” or “in vivo” biological systems.

© 2004 Elsevier B.V. All rights reserved.

Keywords: Mobile phone radiation; Radiofrequency radiation; Acetylcholinesterase

1. Introduction

Diverse studies have been performed with the aim of setting up suitable “in vitro” or “in vivo” tests capable of assessing biological effects induced by electromagnetic fields (EMFs) [1]; however, their conclusions are not consistent. Some authors propose a direct relationship between cellular phone use and a diffuse increase in neurological pathologies, such as panic or depressive syndromes [2], and the most striking of them hypothesize a direct relationship between phone use and brain damage. Conversely, other studies evaluating this possible link have concluded that there is no clear evidence for an excess psychopathological risk [3,4]. It has nevertheless been observed that cellular phone use involves repeated exposure of a relatively constant area of body tissue (i.e., part of the

head) to EMF of variable duration. Considering the microwave intensity and frequency, the duration of exposure is thus important, as it is a conditioning experimental parameter in the determination of possible biological responses.

Most of the energy from a cellular phone antenna is deposited in the skin and outer portion of the brain (cerebral cortex) [5–7]. This energy could locally affect the blood–brain barrier, in which a transient change in permeability could have important health consequences. Lai et al. [8,9] investigated the effects of microwave exposure on cholinergic systems in rat brain showing that, when different microwave power densities were used, it was possible to establish a dose–response relationship for each brain region [10]. They found that, in the rat brain, microwaves activate endogenous opioid neurotransmitters, with morphine-like properties, which are involved in many important physiological and behavioural functions revealing long-term effects such as pain perception and motivation. Daily exposures for 20 min caused an increase in cholinergic activity and a decrease in the concentration

* Corresponding author. Tel.: +39 6 49913957; fax: +39 6 490631.

E-mail address: mario.barteri@uniroma1.it (M. Barteri).

of receptors in the frontal cortex and hippocampus [11]. There was a change in concentration of muscarinic cholinergic receptors, with the direction of change depending on the acute EMF effect. To address the questions raised by prolonged exposure to modulated radiofrequency (RF) transmission, or to study specific end points such as pathological changes in the nervous system, it is necessary to collect information from a wide range of experiments carried out on different biological systems. In this context, to collect reproducible data using different experimental techniques, rigorous protocols, and specific procedures should be carefully planned. Indeed, the interpretation of the EMF radiation-induced alteration, usually performed on animal or tissue experiments, may be complicated by the capacity of the overall biosystem of repairing or masking potential damages occurred at molecular levels. On the contrary, these supposed molecular damages might be more sharply registered by selecting highly purified materials (i.e., enzymes, hormones, or receptors) as biological targets. Our research strategy is to face the same problem at molecular level by selecting specific and highly purified molecular markers (i.e., enzymes, hormones, and receptors). This methodological choice would allow us to identify the RF-induced molecular changes and then to hypothesize the cellular site where the damage had taken place.

The aim of this study was the most basic in this context: to determine the influence of nonthermal exposure to dual band mobile phone radiation on the structure of electric eel acetylcholinesterase (EeAChE; EC 3.1.1.7.). The reason for this choice was both the availability of highly purified enzyme and knowledge of its crystallographic structure. The experimental work was performed examining the overall changes in protein feature. Furthermore, EeAChE's enzymatic activity can easily be tested in "in vitro" preparations, and thus, it provides a suitable model system to study the influence of RF emission on cholinergic activity.

2. Materials and methods

All procedures were performed at 25.0 ± 0.1 °C unless otherwise specified. Highly purified EeAChE was purchased from Sigma (St. Louis, MO, USA), as a suspension containing 5 mg $(\text{NH}_4)_2\text{SO}_4$ per mg of protein. The enzyme was dialyzed against 0.10 M phosphate buffer (K), pH 8, and its purity was checked by HPLC using a Superose 12 HR 10/30 column from Amersham (Pharmacia Biotech), equilibrated and eluted in 0.05 M phosphate buffer containing 0.15 M NaCl–Azide (0.01% NaN_3) with a constant flow of 20 mL h^{-1} . About 100 μL of protein solution (0.70 mg mL^{-1}) was injected in the column and the corresponding elution times were compared to those of protein standards of known molecular mass. Absorbance of the elutes was measured by an UV monitor at a wavelength of 278 nm. Absorbance profiles and chromatographic

parameters were displayed with Win Flow (version 1.2.1). Protein solution concentrations were determined spectrophotometrically at $A_{280 \text{ nm}}$, considering the molar extinction coefficient as $(\epsilon_{280 \text{ nm}} = 52.7 \cdot 10^4 \text{ M}^{-1} \text{ cm}^{-1})$ [12]. Typical EeAChE activity assays were performed by adding 0.02 unit enzyme to 1.0 mL of reaction mixture containing 0.10 M phosphate (K) buffer at pH=8.0, $5.0 \cdot 10^{-4}$ M 5,5' dithio-bis-(2-nitrobenzoate) (DTNB; Sigma, n° cat D 8130) and acetylthiocholine chloride (Sigma, n° cat 420–75) at a concentration of $1.0\text{--}5.0 \cdot 10^{-4}$ M as a substrate [13]. Reaction rates were determined from hydrolysis of acetylthiocholine to acetic acid and thiocholine; this was allowed to react with DTNB and quantified by the absorbance of the newly formed 2-nitro-5-thiobenzoate dianion at 412 nm ($\epsilon = 13600 \text{ M}^{-1} \text{ cm}^{-1}$). SR-SAXS data were recorded at beam line D24 of the DCI Synchrotron facility of L.U.R.E. (Orsay, France). The storage ring was operated using electron beam energy of 1.85 GeV and an injected current of 200 mA. The X-ray wavelength ($\lambda = 1.488 \text{ \AA}$, K-edge of nickel; $\Delta\lambda/\lambda = 10^{-3}$) was selected with a Ge (111) bent crystal. The position-sensitive proportional detector was at a distance of 1574 mm from the sample, with a corresponding channel width of $\Delta K = 1.193 \cdot 10^{-3} \text{ \AA}^{-1}$. Scattering intensities were determined as a function of the modulus of the scattering vector $k = 4\pi \sin\theta/\lambda$, where θ is the scattering angle and λ is the X-ray wavelength. Circular dichroism (CD) spectra were measured and recorded with the Jasco J-715, a spectropolarimeter (Jasco International, Tokyo, Japan) equipped with a computer for processing data. Spectra were recorded in the far-UV region (200–250 nm) using 50 mdeg cm^{-1} sensitivity and 0.1-cm path length QS cuvettes. To reduce the noise/signal ratio, far-UV CD spectra were taken from the average of at least four scans, and were reported as molar ellipticity $[\theta]$ (degree $\text{cm}^2 \text{ dmol}^{-1}$) calculating the protein molarity based on the mean residue molecular weight. Scanning electron micrographs (SEMs) were obtained from a Leo 1450 VP-EDS microscope (Assing), preparing the enzyme solution in double-distilled water to avoid the presence of salts in the specimen, deposited on pyrolytic graphite and analyzed after air-drying. EMF radiations were generated by a GSM dual-band cellular phone and their emission intensity (V m^{-1}) was measured at 5 cm distance from the antenna. A portable PMM 8053 instrument (Country), operating in the frequency range 5–18 GHz and in the field range $0.03 \text{ V m}^{-1}\text{--}100 \text{ kV m}^{-1}$ (precision $0.01\text{--}100 \text{ V m}^{-1}$ and sensitivity $0.1\text{--}1 \text{ V m}^{-1}$) was used for measurements. NMR experiments were carried out on a Bruker 500 at controlled temperature ($310 \pm 0.4 \text{ K}$). Chemical shifts were referenced to external TMS. Spin-lattice relaxation times were determined by standard inversion recovery sequence ($180^\circ\text{--}\tau\text{--}90^\circ$ -acquisition). The relaxation times (T_1) were calculated by fitting the longitudinal magnetization $S(z)$ to Eq. (1):

$$S_z = A - B \exp\left(-\frac{\tau}{T_1}\right) \quad (1)$$

3. Results and discussion

The structural and/or functional effects induced by microwave exposure were studied with a simple but rigorous experimental procedure. Aliquots of the same buffered (PBS 0.1 M, pH 7.4) enzyme solution of identical volumes were placed into glass test tubes. First tube was wrapped in a single thin aluminium foil to screen RF radiations, whereas the remaining tubes were exposed to RF radiations within the range 915–1822 MHz for times varying from 1 to 50 min.

The use of the same EeAChE solutions in identical *T* and *P* conditions guaranteed experimental homogeneity between native and irradiated enzyme, thus minimizing experimental errors due to sample preparation. Spectral and kinetic variations of the enzyme solution were also considered as only due to the structural effect induced by RF exposure.

3.1. Emitted electric field measurements

We used a commercial cellular phone as a source of RF, because we wished to analyze the effect of the whole emissions. However, the correlation between the exposition time and the functional effects implies the characterization of the emitting properties of the phone used. It is known that the emission intensities of commercial mobile phone handsets are different. In light of this, the emission properties of the device were assessed to correlate exposition times and emission-related effects. Moreover, the Specific Absorption Rate (SAR), a generally adopted method of quantifying the energy absorbed by biological tissues, is dependant by electric field measurement according to the equation SAR is expressed in W kg^{-1} and it is given by:

$$SAR = \frac{\sigma E^2}{\rho} (\text{Wkg}^{-1})$$

where σ is the conductivity of the medium, ρ is the density, and $|E^2|$ is the RMS of the electric field intensities. Measured SAR value of the cellular we used (0.51 W kg^{-1}) roughly corresponded to those considered as thermal effect-safe by the International commission on non-ionizing Radiation Protection (ICNIRP). In this study, SAR values were dependent only by $|E^2|$ being both σ and ρ of the diluted sample of EeAChE constant. Therefore, SAR variation were considered to change proportionally to the electric field variation as shown in Fig. 1.

Fig. 1A shows the electric field emissions of the cellular phone recorded operating in both receiving and calling mode. In receiving mode, cellular phone needs a lower amount of energy to be connected, while operating in calling mode oscillations of the emitted electric field increases. All our experiments were carried out operating in receive mode by dialling from a remote phone to the phone positioned at 5 cm far from the enzyme solution and

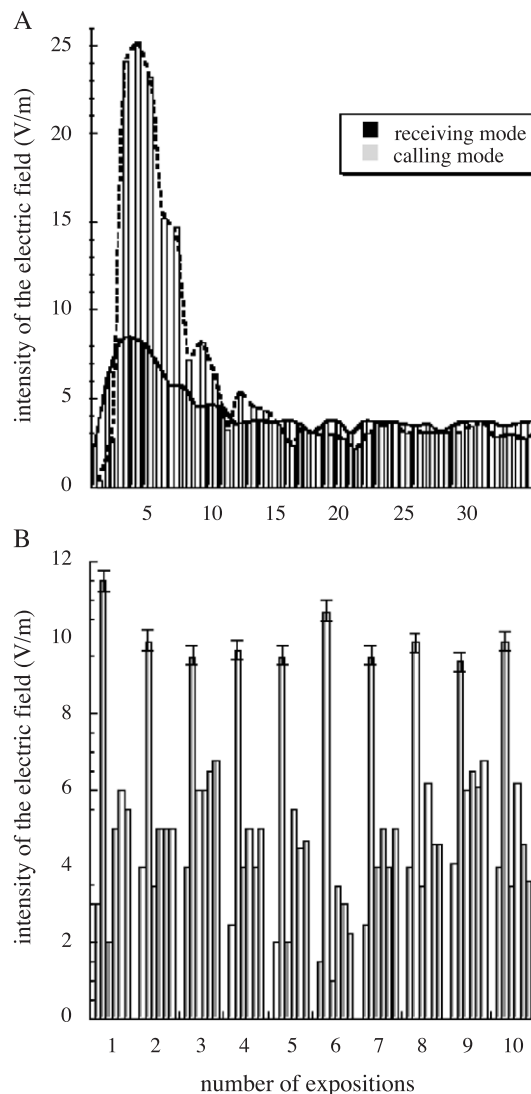


Fig. 1. (A) EMF emission of the cellular phone recorded with PMM 8053 analyzer in both receiving (black histograms) and calling (grey histograms) mode. (B) Sequence of repetitive expositions, of 60 s each, that were utilized to ranging the exposition time between 1 and 50 min.

call was allowed to last for between 1 and 50 min. As soon as the phone we utilized received a call, the emitted intensity of electric field rapidly increased in the first 10 sec, reaching a maximum of 12 V m^{-1} , before decreasing to a lower standby asymptotic value of about 1 V m^{-1} . Panel B of the same figure shows a sequence of (10) repetitive impulses in receiving mode. Each group of histograms represent the higher than 1 V m^{-1} electric field oscillations within 60 seconds. To change the exposition time from 1 to 50 min, we gradually exposed our samples to cycles of 60 sec each.

Despite that, during our performed experiments, we detected no more than $0.2 \text{ }^\circ\text{C}$ of temperature difference we controlled the temperature at $25.0 \pm 0.1 \text{ }^\circ\text{C}$ with a thermostatic bath. Fig. 2 shows a schematic representation of the experimental assembling utilized for these studies.

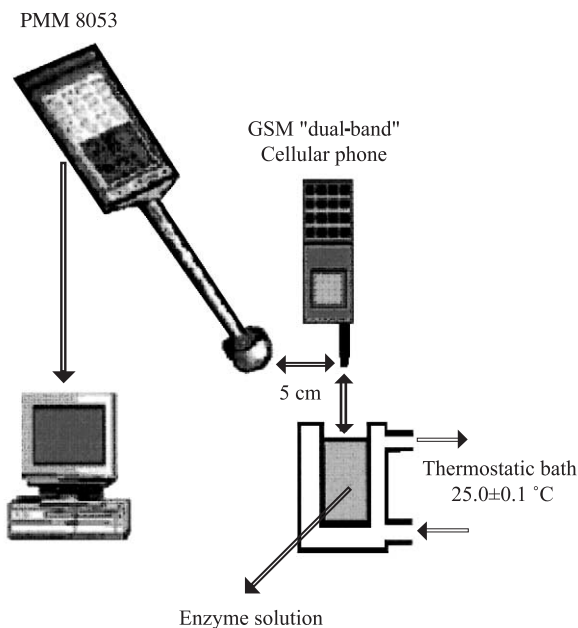


Fig. 2. Schematic representation of the EMF exposition experiments. The temperature of the EeAChE solutions were controlled at 25.0 ± 0.1 °C; the distance between the solution and the cellular phone antenna, as well as the distance between the phone antenna and PMM 8053 analyzer were of 5 cm in all our experiments.

3.2. GPC-HPLC measurements

The EeAChE sample was a soluble collagen-free protein form and it was purified by gel filtration until freed from contaminants (Fig. 3A). This sample was divided into six identical aliquots (1 mL each) of known concentration; one of these was conserved in a test tube protected with aluminium foil to avoid unintentional or accidental exposures to the cellular phone field. The others were exposed to the microwave field of a dual-band cellular phone for 1, 5, 10, 20, and 50 min and then immediately injected into the chromatographic column and analyzed.

At short irradiation times (1–10 min), no significant variations were observed in chromatographic profiles, while after 20-min exposure, the EeAChE sample composition was deeply modified (Fig. 3B). In this case, a newly formed peak corresponding to the enzyme's monomeric form (60 kDa) was observed. An identical profile of the irradiated enzyme solution was recorded after 1-day storage at room temperature, thus demonstrating the irreversibility of the enzyme monomerization. Furthermore, to be sure that the change was due only to the irradiation procedure and not to spontaneous enzyme degradation, HPLC analysis was repeated on the nonirradiated sample that gave a chromatographic profile superimposed to that of Fig. 3A.

3.3. Kinetic enzyme activity measurements

"In vivo", acetylcholinesterase is an extrinsic membrane-bound enzyme responsible for rapid hydrolysis of

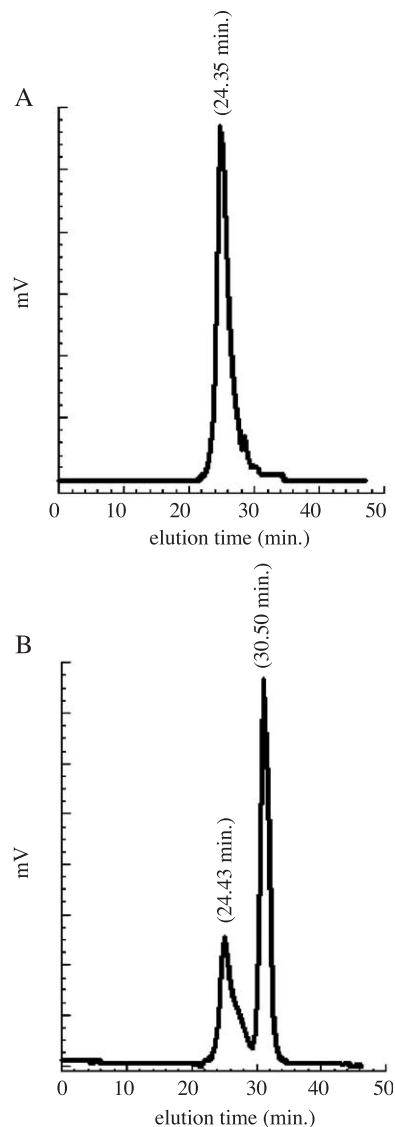
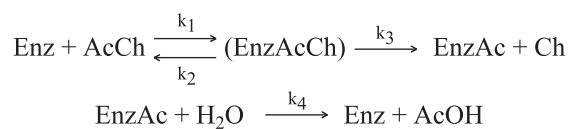


Fig. 3. GPC-HPLC analysis of EeAChE. (A) Elution pattern of purified native enzyme (elution time, 24.35 min). Total of 24 h after its preparation, this enzyme solution, protected with aluminium and stored under Ar atmosphere, gave the same pattern as panel A. (B) Chromatographic elution pattern of enzyme sample after 20 min. exposure to a commercial dual band cellular phone. The chromatogram exhibits both dimer (24.43 min) and monomer (30.50 min) peaks.

the neurotransmitter acetylcholine, liberating choline and acetate within 1 msec of its release at the cholinergic synapses.

The general scheme of enzymic reaction can be summarized as follows:



where: Enz is the enzyme, AcCh is the substrate (acetylcholine), and Ch and AcOH are the products (choline and acetic

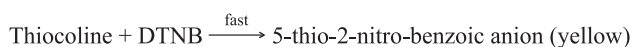
acid, respectively). The reaction rate of the acetylcholine hydrolysis is

$$v = \frac{d[\text{Ch}]}{dt} = \frac{k_3[\text{Enz}]_0[\text{AcCh}]_0}{[\text{AcCh}]_0 + K_M} = \frac{V_M[\text{AcCh}]_0}{[\text{AcCh}]_0 + K_M} \quad (2)$$

The steady-state rate constants are derived from the equations:

$$V_M = k_3[\text{Enz}]_0; \quad K_M = \frac{k_4(k_2 + k_3)}{k_1(k_3 + k_4)}; \quad k_{\text{cat}} = \frac{k_3k_4}{(k_3 + k_4)} \quad (3)$$

Using the experimental irradiation protocol already described, measurements of kinetic enzyme activity were made on both native and irradiated enzyme samples. The enzyme concentration was 0.02 unit mL⁻¹ and the reaction rate was determined using acetylthiocholine as substrate. The concentration of the reaction product (thiocholine) was measured according to the modified Ellman's method [13], based on the following reactions:



The concentration of the yellow anion of 5-thio-2-nitro-benzoic anion ($\epsilon=13\,600\text{ M}^{-1}\text{ cm}^{-1}$ at $\lambda=412\text{ nm}$) allows assessment of hydrolase's activity. Kinetic measurements were carried out to verify the catalytic properties of the enzyme after different exposure times (1, 3, 5, 10, 20, 30, 40, and 50 min) using the native sample as a standard. The initial reaction rate was corrected for spontaneous background acetylthiocholine hydrolysis and it was based on the mean value of at least five runs.

All the solutions exposed up to 10 min provided numerical values that, within experimental error, were very

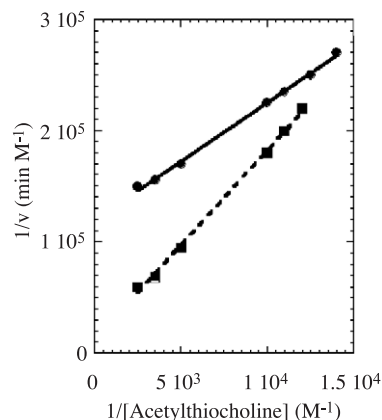


Fig. 4. Lineweaver–Burk plot of enzymatic activity of the same acetylcholinesterase solution before (—) and after (· · ·) exposure to cellular phone radiation. Native and 5-min irradiated samples did not show any appreciable difference in kinetic parameters. On the contrary, as soon as exposure time increased, significant differences were found in V_{max} , K_M , and k_{cat} kinetic parameters which had had a continuous irradiations of 20 min (Table 1).

Table 1

Kinetic activity parameters of native and irradiated (20 min) EeAChE calculated by Lineweaver–Burk plot (Fig. 4)

	V_M ($\mu\text{M L}^{-1}\text{ sec}^{-1}$)	K_M ($\mu\text{M}^{-1}\text{ L}$)	$k_{\text{cat}} 10^{-6}$ (sec^{-1})
Native	8.5 ± 1.1	84.0 ± 11.8	1.1 ± 0.1
Irradiated	80.6 ± 12.9	1372.1 ± 226.4	4.2 ± 0.6

Values represent the mean of three different experiments and their variability range.

similar to those of the native enzyme, while larger exposition time showed a considerable increase in the kinetic parameters. Fig. 4 compares the double reciprocal Lineweaver–Burk plots of the inverse initial reaction rate ($1/v$) against the inverse of substrate concentration ($1/[S]$) for the native sample and the same enzyme after 20-min exposure. To reveal the dose–response relationship and any progressive accumulation mechanism of energy from the cellular phone's antenna, K_M , V_M , and k_{cat} values of each exposed sample were calculated (Table 1). Table 1 shows these figures with the range of their variability observed following three different exposures of 20 min each. Longer irradiation times (20–50 min) were not associated with further modification of such parameters.

This kind of exposition to the cellular phone deeply modified the enzymic activity of EeAChE and might serve to explain the increase of cholinergic activity observed in mice after twenty minutes irradiation. The same authors report a decrease in the concentration of receptors in the frontal cortex and hippocampus.

3.4. Circular dichroism studies

At this stage of our studies, two questions needed to be addressed: first, why do kinetic constants change after irradiation? Second, can RF provoke conformational modifications in the secondary and tertiary protein structure? To answer these questions was particularly important because catalytic activity of enzymes may change even if only minor structural modifications occur in the active site. Circular dichroism spectroscopy (CD) is a powerful tool for revealing any conformational change to the protein structure. The intensity of the far-UV CD signal ($190 < \lambda < 250\text{ nm}$) is sensitive to each type of ordered secondary structure, as shape and intensity of the near-UV CD spectrum ($250 < \lambda < 360\text{ nm}$) are related to the tertiary structure of the protein. Fig. 5 shows a comparison between the far-UV CD spectra from 190 to 250 nm of native EeAChE (protected with aluminium) and samples exposed to mobile phone radiation up to 50 min. Surprisingly, we obtained highly reproducible spectra which revealed that microwaves did not alter the secondary structure of the enzyme. Similar result was obtained in the far-UV CD region (data not shown) showing that modification of the enzymic activity did not concern conformational changes, but can be attributed to the monomerization of the protein revealed by mean of GPC-HPLC measurements.

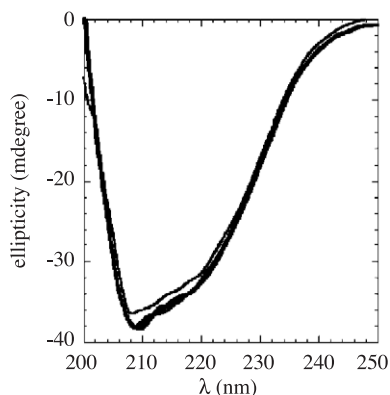


Fig. 5. Circular dichroism spectra of EeAChE solution (0.6 mg mL^{-1}) (native and irradiated for up to 50 min). Molar ellipticities are not significantly affected by irradiation, showing that microwaves did not induce any conformational changes to the secondary protein structure.

3.5. Synchrotron radiation small-angle X-ray scattering (SR-SAXS)

The opportunity of performing SAXS measurements using synchrotron radiation (SR) facilities allowed us to collect highly defined scattering measurements from diluted protein solutions ($2\text{--}6 \text{ mg mL}^{-1}$). In these experiments, it should be, however, considered that the SR X-ray beam is highly collimated with a very high brilliance, which, in aqueous solution, can produce free radicals capable of damaging biological samples [14]. It was thus necessary to adopt suitable experimental procedures to avoid this drawback as far as possible. We collected scattering data using a flow cell with a flow of $3 \mu\text{L sec}^{-1}$ to reduce exposure to the X-ray beam. As the solution volume exposed to the beam was about $3\text{--}4 \mu\text{L}$, this flow guaranteed an efficient renewal of the protein solution exposed to the X-ray beam and was fast enough to prevent protein damage. Fig. 6A compares the scattering curves of native EeAChE and of the enzyme irradiated for 20 min collected under continuous flux regime. The native sample shows the typical trend of monodisperse protein solution, with a radius of gyration (R_g) of $43.6 \pm 0.3 \text{ \AA}$, calculated from the slope of the linear plot $\ln I(k)$ vs. k^2 of Guinier and Fournet's equation [15]:

$$\ln I(k) = \ln I_0 - \frac{1}{3} R_g^2 k^2 \quad (4)$$

where: $k=4\pi(\sin(\theta))/(\lambda)$ and I_0 is the scattering intensity at zero angle ($\theta=0$; $k=0$). For a given solute–solvent system, with a suitable density contrast difference, R_g is a measure of both particle elongation and the internal arrangement of different scattering densities. I_0/c (c =sample concentration, defined by the EeAChE protein concentration) is proportional to the relative molecular mass (M_r). Radii of gyration were calculated in the range $0.03 \leq k \text{ (\AA}^{-1}\text{)} \leq 0.05$ of the scattering vector where, for spherical macromolecules, the approximation of Guinier's Law is valid up to a kR_g of 1.3 and approximate up to $2 kR_g$. For the native enzyme, the slope of the linear part of the plots $\ln[I(k)k^2]$ vs. k^2 and

$\ln[I(k)k^2]$ vs. k^2 provided radii values of the cross-section ($R_c=29.8 \pm 0.4 \text{ \AA}$) and of the thickness ($R_t=20.5 \pm 0.6 \text{ \AA}$).

After irradiation, scattering intensity increased significantly and shifted towards higher values of the scattering vector (k). This trend suggested the formation of EeAChE hydrogels from the assembly of highly hydrated protein molecules. In this case, centrifugation ($4000 \times g$ for 5 min) gave hydrogel separation while native enzyme sample did not, thus confirming that cellular phone RF caused a hydrogel pattern of protein. To better clarify this point and to obtain more information about the size, compactness and shape of both native and exposed scattering molecule, we

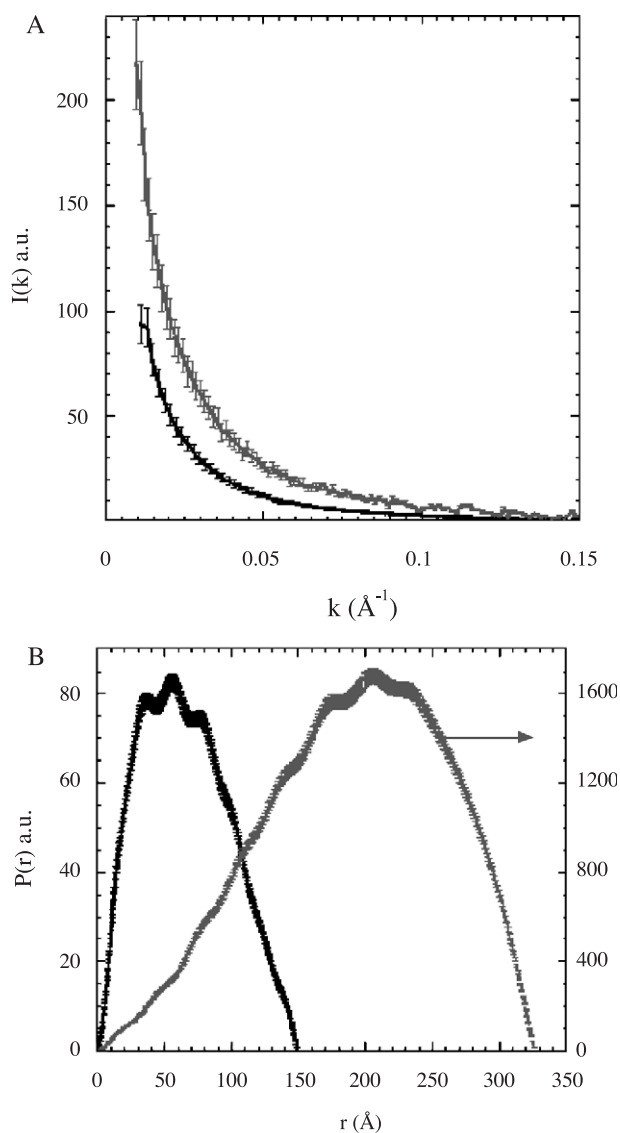


Fig. 6. (A) SR-SAXS measurements of native and irradiated EeAChE. Scattering measurements were collected using a flux cell to avoid X-ray damage to the sample. The same enzyme solution was used to collect the scattering intensities of both native (black line) and irradiated (grey line) sample. (B) Distance distribution function ($P(r)$) trends of the native (black line) and irradiated (grey line) samples. According to Eq. (5), calculations were carried out using scattering data of panel A.

used scattering data to calculate pair distance distribution function ($P(r)$) (Eq. (5)).

$$P(r) = \frac{1}{2\pi^2} \int_0^\infty I(k)rk\sin(rk)dk \quad (5)$$

Fig. 6B illustrates a comparison of the $P(r)$ vs. r plots of the same enzyme solution before and after exposition. Irradiated sample resulted deeply modified because of the presence of a hydrogel composed of monomeric protein molecules and water, stabilized by strong interparticle interactions. This peculiar assembling of the enzyme may cause the observed alterations of kinetic parameters because water distribution within the protein dominion is critical for the substrate diffusion altering the enzyme-substrate interaction.

3.6. Environmental scanning electron microscopy (ESEM)

Because the main consequence of the RF irradiation was the formation of detectable hydrogel, specimens of native and irradiated EeAChE were collected and analyzed by ESEM. These techniques have the advantage of giving real pictures with a resolution, providing valuable information on the protein features. Fig. 7 shows micrographs at the same magnification of the protein before and after cellular phone exposure, revealing marked structural differences: native enzyme appears as a nonordered coagulated sample concentrated during air-drying. Conversely, the irradiated enzyme appears as a highly orientated sample with an evident and regular periodic pattern, generated by the RF emission of the cellular phone.

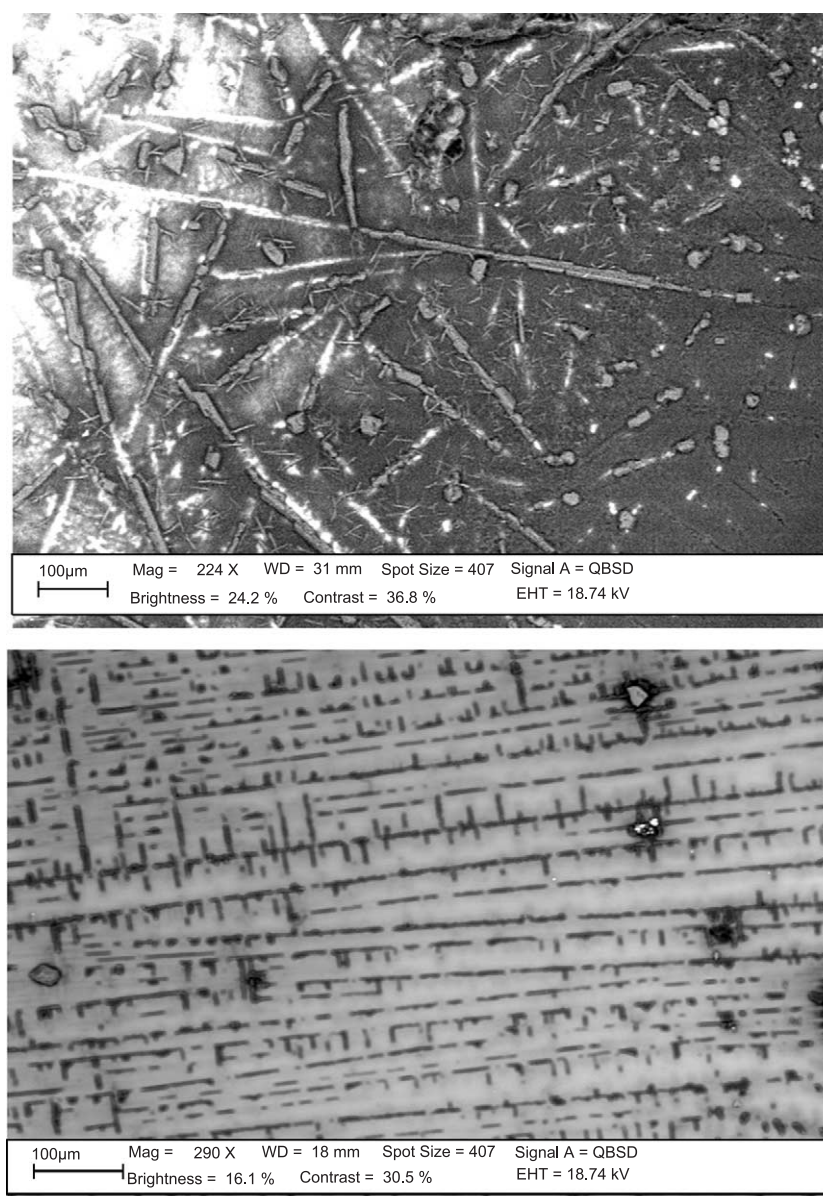


Fig. 7. Scanning electron microscopy EeAChE images before (top) and after (bottom) cellular phone irradiation. The enzyme solution (0.6 mg mL^{-1}) was prepared in double-distilled water; $20 \text{ }\mu\text{L}$ of native and exposed solution were deposited on graphite and left to dry.

In explaining these experimental results, careful consideration should be given to the fundamental contribution by Clifford et al. [16] on the relationship between three-dimensional (3D) structures of cholinesterases from various species and their physical and chemical properties. A peculiar characteristic of acetylcholinesterases is the presence of a large negative potential near the active site dominion (gorge), due to the presence of negatively charged residues located at the entrance, midway down and near the gorge base. This charged group distribution leads to an electrostatic field, whose potential was calculated solving the Poisson–Boltzmann equation by means of the finite difference method [17] implemented in the Delphi algorithm [18]. In a protein, the nonhomogeneous distribution of their partial atomic charges may be quantified by the position-dependent first moment of charge distribution $\mu = \sum r_i q_i$, where r_i is the position vector and q_i is the partial charge located on each atom i in the molecule. Cholinesterases have a rather strong first moment of 800–1800 Debye roughly aligned along the gorge axis, so that a positive-charged substrate will be drawn to the active site by its electrostatic field, creating a selective and efficient substrate-binding site interaction. In the EeAChE monomer, the first moment calculated using PDB crystallographic structure (PDB ID code 1C2B) through PDB dipole program [19,20] is 1061 Debye, while for the dimer (PDB ID code 1EEA), it is 1799 Debye.

When a cellular phone sends or receives a signal for a standard call, a fast and large variation in the electric field takes place. We measured relative electric field variation at 5 cm from the antenna with the phone during a normal call. On this basis, our results suggest that the strong EeAChE first moment, created by the charge distribution of the protein, is sensitive to fluctuation of the RF emission from the cellular phone. Moreover, also the dipolar molecules of the solvent can be perturbed, because water molecules give rise to an anisotropic long-range potential that, in the presence of ionic species, is generally associated with a high degree of rotational inelasticity [21].

3.7. NMR spin-lattice relaxation rate (T_1)

The EMF associated to the RF emission may perturb the intermolecular interaction between water solvent and EeAChE polypeptide chain, causing the dimer dissociation and the formation of stable hydrogel of monomeric enzyme molecules. Hydrogels are 3D complex systems of solute and water molecules forming a tangle network. Three types of water have been classified in hydrophilic gels: nonfreezing or bound water, interfacial or intermediate water, and free water. The rate, at which the water diffuses within hydrophilic dominions to form the gel layer, is the major factor that determines physical and chemical characteristic of the whole system. Thus, characterization of the types of water existing within the monomeric EeAChE hydrogel was fundamental to recognize the changes in the enzyme

Table 2

Water H^1 NMR relaxation times (T_1) of native and irradiated EeAChE

Sample	T_1 (ms)
Solvent ($H_2O+10\% D_2O$)	2983 ± 27
Native EeAChE	470 ± 25
Irradiated EeAChE (20 min)	260 ± 32
Irradiated EeAChE (50 min)	220 ± 38

Each value is the average of five experimental T_1 determination.

structural and kinetic properties. NMR is an appropriate technique for detailed studies of the structure, mobility, and hydration properties of various polyelectrolyte systems, such as hydrogels of proteins in water solution. The nuclear spin relaxation of solvent nuclei (e.g., water protons) is usually enhanced in the presence of proteins and/or in the presence of a paramagnetic substance. In pure water, proton relaxation is governed by a dipole–dipole mechanism between protons, modulated by the reorientation motion of the molecule. Small molecules reorient rapidly (i.e., τ is small) and slow relaxation results. If a water molecule is “bound” to a large diamagnetic molecule, as a protein, protons relaxation is enhanced with respect to bulk water, due to the slower rotational time. Table 2 summarizes H^1 NMR spin-lattice relaxation times (T_1) of pure solvent, of native (not exposed) EeAChE sample and those of the same sample after 20 and 50 min of exposition. Interestingly enough, the relaxation times at 20 and 50 min were very similar, indicating that the jellification was a complete and a time-independent process within this period. Measurements were carried out using enzyme in phosphate buffer containing 10% D_2O . Each relaxation time T_1 was the average value calculated on five experimental measurements. The decrease in selective relaxation times is consistent with an exchange between protein and free bulk environment [22,23]. Data of Table 2 lead to the conclusion that the hydration state of the protein mostly influences the water proton NMR spin-lattice relaxation rate ($1/T_1$). Exposed enzyme sample exhibited a further decrease of the T_1 , confirming an increase of bound water fraction associated with a hydrogel state [24].

4. Conclusions

The tremendous increase in the use of cellular telephones strongly stimulated our interest in studying the “in vitro” interaction between amplitude modulated radio frequencies and proteins of different species. To date, there has been no direct scientific evidence that non-ionizing radiation can lead to any effect on enzymes and proteins of the central nervous system (CNS). This paper first demonstrates that cellular phone emissions affect the structural and biochemical characteristics of an important CNS enzyme. The EeAChE irradiation determined an irreversible monomerization of the protein accompanied by a significant change in the enzyme activity. SR-SAXS

measurements provided data on the association of newly formed monomers into a soluble hydrogel. Jellification was confirmed by the variation of $^1\text{H-NMR}$ spin-lattice relaxation times (T_1) values. Further evidences of this process were observed by Echo Scanning Electron Microscopy observations.

We would underline that these results were obtained by using a commercial cellular phone to reproduce the reality of the human exposition. Furthermore, this experimental procedure brought about unexpected effects collected practically without experimental errors because they were obtained comparing native and irradiated sample of the same enzyme solution. In these kinds of studies on the use of commercial phones as source of RF, the variability of the RF and intensity might be considered a limiting condition. However, commercial phones are indeed the most common RF sources in the human exposition in everyday life. In light of this, this paper was undertaken to study the effect of the overall phone emissions on a well defined biological target such as AChE. Such an experimental model proved to be reproducible when irradiation time exceeded 20 min at the enzyme concentration we used. Indeed, this time corresponded to the complete monomerization and jellification of the sample as shown by GPC-HPLC, T_1 -NMR, and SR-SAXS measurements. It is known that various cellular phones are characterized by highly different emission properties which are specific both of the manufacturing and of their operating mode. Therefore, the effect on EeAChE similar to those described in this paper are likely to be observed using different instruments although different irradiation times could be necessary to get the same complete monomerization of the target enzyme molecule.

These results cannot be used to conclude that the cellular phone emission can lead to hazardous effect for the human health, but they may be a significant model to verify these effects on other biological systems.

Acknowledgements

This study was financed by MURST and by the Training and Mobility of Researchers (TMR) Program of the European Community for the SAXS experiments at L.U.R.E. (Fr). The authors thank Dr. Patrice Vachette for his collaboration during the SAXS experiments and Prof. Maurizio Delfini for his help in carrying out NMR measurements.

References

- [1] R.-D. Saunders, C.-I. Kowalczyk, Z.-J. Sienkiewicz, Biological effects of exposure to non-ionizing electromagnetic fields and radiation, Radiofrequency and microwave radiation. National Radiological Protection Board, Chilton, NRPB-R240, HMSO, London, 1991.
- [2] D. Leszczynski, S. Joenväärä, J. Reivinen, R. Kuokka, *Differentiation* 70 (2002) 120–129.
- [3] IEEE Standard for safety levels with respect to human exposure to radiofrequency electromagnetic field, 3 kHz to 300 GHz. Institute of Electrical and Electronic Engineers, IEEE C95.1-1991, IEEE, 345 East 47th. Street, New York (1992).
- [4] NPRB, Board statement on restrictions on human exposure to static and time varying electromagnetic field and radiation, Natl. Radiol. Board, Doc. NRPB 4 (5) (1993) 1–63.
- [5] P.-J. Dimbylow, J.-M. Mann, *Phys. Med. Biol.* 39 (1994) 1527–1553.
- [6] L. Martens, J. DeMoerloose, C. DeWagter, D. DeZutter, *Radio Sci.* 30 (1995) 415–420.
- [7] B.-K. Chang, A.-T. Huang, W.-T. Joines, R.-S. Kramer, *Radio Sci.* 17 (1982) 165–168.
- [8] H. Lai, A. Horita, C.-K. Chou, A.-W. Guy, *J. Neurochem.* 48 (1987) 40–45.
- [9] H. Lai, A. Horita, A.-W. Guy, *Bioelectromagnetics* 9 (1988) 355–362.
- [10] H. Lai, M.-A. Carino, A. Horita, A.-W. Guy, *Bioelectromagnetics* 10 (1989) 203–209.
- [11] W.-R. Adey, C.-V. Byus, C.-D. Cain, Second World Congress for Electricity in Biology and Medicine. Bologna, Italy, June 8–13, 1997.
- [12] K.-J. Kremzner, P.-A. Wilson, *Biochemistry* 3 (1964) 1902–1910.
- [13] P.-W. Riddles, R.-L. Blackeley, B. Zerner, *Anal. Biochem.* 94 (1979) 75–81.
- [14] M. Weik, B.-G. Raimond, G.-K. Ravelli, S. McSweeney, M.-L. Raves, M. Harel, P. Gros, I. Silman, J. Kroon, J.-L. Sussman, *Proc. Natl. Acad. Sci. U. S. A.* 97 (2000) 623–628.
- [15] A. Guinier, G. Fournet, *Small Angle Scattering of X-rays*, Wiley, New York, 1955.
- [16] E.-F. Clifford, S.-A. Botti, S. Lifson, I. Silman, J.-L. Sussman, *J. Mol. Graph. Model.* 15 (1997) 318–327.
- [17] J. Warwicker, H.C. Watson, *J. Mol. Biol.* 157 (1982) 671–679.
- [18] M.K. Gilson, K.A. Sharp, B.H. Homig, *J. Comput. Chem.* 9 (1988) 327–335.
- [19] <http://bioinformatics.weizmann.ac.il/dipol/> Web Server to Calculate Dipole Moments of Proteins Clifford Felder and Joel Sussman, Dept. of Structural Biology Weizmann Institute, 761000 Rehovot, Israel.
- [20] R.A. Laskowski, E. Hutchinson, M. Gail, A.D. Wallace, C. Andrew, M.-L. Jones, et al. PDB-Sum: a Web-based database of summaries and analyses of all PDB structures 488–490.
- [21] F.-A. Gianturco, A. Palma, E. Semprini, F. Stefani, *J. Phys., B At. Mol. Opt. Phys.* 24 (1991) 4531–4552.
- [22] A. Blinc, G. Lahajnar, R. Blinc, A. Zidanšek, A. Sepe, *Magn. Reson. Med.* 14 (1990) 105–122.
- [23] D.-G. Gadian, *Nuclear Magnetic Resonance and its Applications to Living Systems*, The Alden Press, Oxford, England, 1984.
- [24] R. Blinc, V. Rutar, I. Zupančič, A. Zidanšek, G. Lahajnar, *J. Slak, Appl. Magn. Reson.* 9 (1995) 193–216.